Peer-reviewed version available at Mathematics 2019, 7, 216; doi:10.3390/math7030216

# An efficient local formulation for time–dependent PDEs

Imtiaz Ahmad[a], Muhammad Ahsan[a,b], Masood Ahmad[b], Zaheer-ud-Din[b] and Poom Kumam[c,*]

[a]Department of Mathematics, University of Swabi, Swabi, Pakistan

[b]Department of Basic Sciences, University of Engineering and Technology, Peshawar, Pakistan

[d]KMUTTFixed Point Research Laboratory, Room SCL 802 Fixed Point Laboratory, Department of Mathematics, Science Laboratory Building, Faculty of Science, King Mongkut's University of Technology Thonburi (KMUTT), 126 Pracha-Uthit Road, Bang Mod, Thrung Khru, Bangkok 10140, Thailand

**Abstract**

In this paper, a local meshless method (LMM) based on radial basis functions (RBFs) is utilized for the numerical solution of various types of PDEs, due to the flexibility with respect to geometry and high order of convergence rate. In case of global meshless methods, the two major deficiencies are the computational cost and the optimum value of shape parameter. Therefore, research is currently focus towards localized radial basis function approximations, as the local meshless method is proposed here. The local meshless procedures is used for spatial discretization whereas for temporal discretization different time integrators are employed. The proposed local meshless method is testified in terms of efficiency, accuracy and ease of implementation using regular and irregular domains.

**Keywords:** Local meshless method, RBFs, Irregular domains, Kortewege-de Vries types equations, reaction-diffusion Brusselator system.

## 1 Introduction

Most of the problems in real world can be described by partial differential equations (PDEs). In this regard one of the important PDE model is fifth order Kortewege-de Vries model. Its general exact solution is not known whereas the exact solution for particular case of solitary waves can be found in [48]. To solve this model numerically, serval methods can be found in literature such as finite–deference scheme [13], modified ADM [8], decomposition method [27], Homotopy perturbation transform method [18] and a comparative study of Crank-Nicolson method and ADM [21].

The general seventh order Kortewege-de Vries equation [34] which is used to discuss structural stability under singular perturbation of standard KdV equation. Several authors have paid attention to solve the seventh order KdV equation [12, 14, 40].

Generalized Burgers' Huxley equation [35] is used to describe the interaction between convection effects, reaction mechanisms and diffusion transports. In general it is difficult and sometimes impossible to get exact solution of such type nonlinear PDE. Researchers employed different numerical techniques which include discrete Adomian decomposition method [4], Haar wavelet method [11], Adomian decomposition method [24], meshless collocation method based on RBF

[29] and local meshless method [10] for the solution of Burgers' Huxley equation. The Huxley model equation [23] describes nerve pulse propagation in nerve fibres and wall motion in liquid crystals [7]. Numerical solution of Huxley equation can be found in [5, 24, 29] and the references therein. Generalized Burgers' Fisher equation [15], describe the propagation of a mutant gene. Different numerical methods have been used for numerical solution of this model, such as meshless collocation method [29], ADM [24], VIM [32], modified pseudo spectral method [25] and modified cubic B–spline functions collocation method [31].

The Fitzhugh-Nagumo (FN) equation has numerous applications in different fields such as branching brownian motion process, flame propagation, neurophysiology, logistic population growth and nuclear reactor theory [9]. Numerical solution of FN equation can be found in [1, 20, 26, 31].

Hirota-Satsuma introduced the nonlinear coupled Kortewege–de Vries equations [22]. This model has numerous applications in physical sciences. In the last decade, researchers have used various numerical techniques for the solution of this model equations. These include RBFs collocation (Kansa) method [39], meshless RBFs method of lines [19], variational iteration method [6] and spectral collocation method [28]. The Hirota–Satsuma coupled KdV system [47] has been solved by different numerical methods given in [17, 28, 43] and the references therein.

The Brusselator system is one of the essential reaction–diffusion model equation. This model explain the mechanism of a chemical reaction–diffusion with non–linear oscillations [30, 42]. Numerical solution of the model can be found in [2, 38, 45, 46].

In the last few years, it is observed that meshless methods have been extensively employed for numerical simulations of different types of PDEs [37, 39, 41]. Meshless methods reduce complexity caused due to dimensionality to a large extent which is being faced in the carrying out of conventional methods like finite-element and finite-difference procedures. Meshing in the case of complicated geometries is another cause for the growing demand of meshless methods.

It is noticed that global meshless methods faced the problem of dense ill-conditioned matrices and finding optimum value of the shape parameter. To avoid these problems, local meshless methods are used as alternative to get a stable and accurate solution for the PDE models [3, 37].

## 2 Partial differential equation models

A short description of PDE models on a bounded domain with corresponding initial and boundary conditions are given in this section. These include; one-dimensional fifth order Lax's-Kortewege-de Vries, seventh order Lax's-Kortewege-de Vries, generalized Burgers'-Huxley, Huxley, generalized Burgers' Fisher, Fitzhugh-Nagumo, coupled Kortewege-de Vries, Hirota-Satsuma coupled Kortewege-de Vries equations and two-dimensional reaction-diffusion Brusselator equations.

The 1D fifth order Kortewege-de Vries equation [8],

$$U_t + aU^2U_x + bU_xU_{xx} + cUU_{xxx} + dU_{xxxxx} = 0, \tag{1}$$

where $a$, $b$, $c$, $d$ are real constants and in this paper we have taken $a = b = 30$, $c = 10$, and $d = 1$. The 1D seventh order Kortewege-de Vries equation [12],

$$U_t + aU^3U_x + bU_x^3 + cUU_xU_{xx} + dU^2U_{xxx} + eU_{xx}U_{xxx} + fU_xU_{xxxx} + gUU_{xxxxx} + U_{xxxxxxx} = 0, \tag{2}$$

where $a$, $b$, $c$, $d$, $e$, $f$, $g$ are real constants and we have taken $a = 140$, $b = 70$, $c = 280$, $d = 70$, $e = 70$, $f = 42$, $g = 14$.

Preprints (www.preprints.org) | NOT PEER-REVIEWED | Posted: 31 January 2019 doi:10.20944/preprints201901.0330.v1

Peer-reviewed version available at Mathematics 2019, 7, 216; doi:10.3390/math7030216

The 1D generalized Burgers'-Huxley equation [4, 11, 24, 29, 35],

$$U_t + \alpha U^\delta U_x - U_{xx} - \beta U(1 - U^\delta)(U^\delta - \gamma) = 0, \tag{3}$$

where $\alpha$, $\beta \geq 0$, $\delta > 0$, $\gamma \in (0, 1)$ are constants.
The 1D Huxley equation [5, 24, 29]

$$U_t - U_{xx} - \beta U(1 - U)(U - \gamma) = 0, \tag{4}$$

where $\beta$ and $\gamma$ are constants.
The 1D generalized Burgers' Fisher equation [24, 29],

$$U_t + \alpha U^\delta U_x - U_{xx} - \beta U(1 - U^\delta) = 0, \tag{5}$$

where $\alpha$, $\beta$ and $\delta$ are constants.
The 1D Fitzhugh-Nagumo (FN) equation [9, 16, 26, 33],

$$U_t - U_{xx} + U(1 - U)(\rho - U) = 0, \tag{6}$$

where $\rho$ is a constant.
The 1D coupled Kortewege-de Vries equation [19, 22, 28, 39],

$$\begin{aligned} U_t + 6\alpha U U_x - 2\gamma V V_x + \alpha U_{xxx} = 0, \\ V_t + 3\beta U V_x + \beta V_{xxx} = 0, \end{aligned} \tag{7}$$

where $\alpha$, $\beta$ and $\gamma$ are real parameters.
The 1D Hirota-Satsuma coupled KdV system of equations [28, 47],

$$\begin{aligned} U_t - \frac{1}{2} U_{xxx} + 3UU_x - 3VW_x - 3WV_x = 0, \\ V_t + V_{xxx} - 3UV_x = 0, \\ W_t + W_{xxx} - 3UW_x = 0. \end{aligned} \tag{8}$$

The 2D reaction-diffusion Brusselator system of equations [38, 46]

$$\begin{aligned} U_t - \beta - U^2 V + (\alpha + 1)U - \gamma(U_{xx} + U_{yy}) = 0, \\ V_t - \alpha U + U^2 V - \gamma(V_{xx} + V_{yy}) = 0, \end{aligned} \tag{9}$$

where $\alpha$, $\beta$ and $\gamma$ are constants.

## 3 Local meshless numerical scheme

To pursue the LMM [36,37], we approximate the derivatives of $U(x, t)$ at the center $x_p$ by the function values at a set of nodes in the neighborhood of $x_p$, $\{x_{p_1}, x_{p_2}, x_{p_3}, ..., x_{p_{n_j}}\} \subset \{x_1, x_2, \ldots, x_{N^n}\}, n_p \ll N^n$, where $n = 1$, $n = 2$ for one and two dimensional case respectively.

$$U^{(m)}(x_p) \approx \sum_{k=1}^{n_p} \lambda_k^{(m)} U(x_{p_k}),\ p = 1, 2, \ldots, N^n. \tag{10}$$

Preprints (www.preprints.org) | NOT PEER-REVIEWED | Posted: 31 January 2019 doi:10.20944/preprints201901.0330.v1

Peer-reviewed version available at Mathematics 2019, 7, 216; doi:10.3390/math7030216

To find the corresponding coefficient $\lambda_k^{(m)}$, radial basis function $\phi(\|x - x_l\|)$ can be substituted into equation (10)

$$\phi^{(m)}(\|x_p - x_l\|) = \sum_{k=1}^{n_p} \lambda_{p_k}^{(m)} \phi(\|x_{p_k} - x_l\|),\ l = p_1, p_2, \ldots, p_{n_p}. \tag{11}$$

Equation (11) in matrix form

$$\begin{bmatrix} \phi_{p_1}^{(m)}(x_p) \\ \phi_{p_2}^{(m)}(x_p) \\ \vdots \\ \phi_{p_{n_p}}^{(m)}(x_p) \end{bmatrix} = \begin{bmatrix} \phi_{p_1}(x_{p_1}) & \phi_{p_2}(x_{p_1}) & \cdots & \phi_{p_{n_p}}(x_{p_1}) \\ \phi_{p_1}(x_{p_2}) & \phi_{p_2}(x_{p_2}) & \cdots & \phi_{p_{n_p}}(x_{p_2}) \\ \vdots & \vdots & \ddots & \vdots \\ \phi_{p_1}(x_{p_{n_p}}) & \phi_{p_2}(x_{p_{n_p}}) & \cdots & \phi_{p_{n_p}}(x_{p_{n_p}}) \end{bmatrix} \begin{bmatrix} \lambda_{p_1}^{(m)} \\ \lambda_{p_2}^{(m)} \\ \vdots \\ \lambda_{p_{n_p}}^{(m)} \end{bmatrix}, \tag{12}$$

where

$$\phi_l(x_k) = \phi(\|x_k - x_l\|),\ l = p_1, p_2, \ldots, p_{n_p}, \tag{13}$$

for each $k = p_1, p_2, \ldots, p_{n_p}$.
The above equation in matrix notation

$$\mathbf{\Phi}_{n_p}^{(m)} = \mathbf{A}_{n_p} \boldsymbol{\lambda}_{n_p}^{(m)}, \tag{14}$$

where

$$\mathbf{\Phi}_{n_p}^{(m)} = \begin{bmatrix} \phi_{p_1}^{(m)}(x_p) & \phi_{p_2}^{(m)}(x_p) & \cdots & \phi_{p_{n_p}}^{(m)}(x_p) \end{bmatrix}^T$$

$$\mathbf{A}_{n_p} = \begin{bmatrix} \phi_{p_1}(x_{p_1}) & \phi_{p_2}(x_{p_1}) & \cdots & \phi_{p_{n_p}}(x_{p_1}) \\ \phi_{p_1}(x_{p_2}) & \phi_{p_2}(x_{p_2}) & \cdots & \phi_{p_{n_p}}(x_{p_2}) \\ \vdots & \vdots & \ddots & \vdots \\ \phi_{p_1}(x_{p_{n_p}}) & \phi_{p_2}(x_{p_{n_p}}) & \cdots & \phi_{p_{n_p}}(x_{p_{n_p}}) \end{bmatrix}$$

$$\boldsymbol{\lambda}_{n_p}^{(m)} = \begin{bmatrix} \lambda_{p_1}^{(m)} & \lambda_{p_2}^{(m)} & \cdots & \lambda_{p_{n_p}}^{(m)} \end{bmatrix}^T.$$

From equation (14),

$$\boldsymbol{\lambda}_{n_p}^{(m)} = \mathbf{A}_{n_p}^{-1} \mathbf{\Phi}_{n_p}^{(m)}. \tag{15}$$

By substituting equation (15) into equation (10),

$$U^{(m)}(x_p) = (\boldsymbol{\lambda}_{n_p}^{(m)})^T \mathbf{U}_{n_p}, \tag{16}$$

where

$$\mathbf{U}_{n_p} = \left[ U(x_{p_1}), U(x_{p_2}), \ldots, U(x_{p_{n_p}}) \right]^T. \tag{17}$$

### 3.1 1D fifth order Kortewege-de Vries equation

The 1D fifth order Kortewege-de Vries equation (1) can be written as

$$U_t = -(aU^2 U_x + bU_x U_{xx} + cUU_{xxx} + dU_{xxxxx}),\quad x \in \Omega,\ \ t \geq 0, \tag{18}$$

subject to initial and boundary conditions

$$U(x, 0) = f(x),\quad x \in \Omega, \tag{19}$$

Preprints (www.preprints.org) | NOT PEER-REVIEWED | Posted: 31 January 2019 doi:10.20944/preprints201901.0330.v1

Peer-reviewed version available at Mathematics 2019, 7, 216; doi:10.3390/math7030216

$$U(x,t) = f_1(t), \;\; U(x,t) = f_2(t), \quad x \in \partial\Omega. \tag{20}$$

where $a$, $b$, $c$ and $d$ are constants.

Now, Applying the LMM to equation (18) we get,

$$\frac{dU_p}{dt} = -(aU_p^2(\boldsymbol{\lambda}_{n_p}^{(1)})^T\mathbf{U}_{n_p} + b((\boldsymbol{\lambda}_{n_p}^{(1)})^T\mathbf{U}_{n_p})((\boldsymbol{\lambda}_{n_p}^{(2)})^T\mathbf{U}_{n_p}) + cU_p(\boldsymbol{\lambda}_{n_p}^{(3)})^T\mathbf{U}_{n_p} + d(\boldsymbol{\lambda}_{n_p}^{(5)})^T\mathbf{U}_{n_p}), \; p = 2,3,\ldots,N-1. \tag{21}$$

The semi-discretized model equation (21) with boundary conditions (20) is given as follows

$$\frac{d\mathfrak{U}}{dt} = -(a\;\mathfrak{U}^2 * (\mathbf{\Lambda}^{(1)}\mathfrak{U}) + b(\mathbf{\Lambda}^{(1)}\mathfrak{U}) * (\mathbf{\Lambda}^{(2)}\mathfrak{U}) + c\;\mathfrak{U} * (\mathbf{\Lambda}^{(3)}\mathfrak{U}) + d(\mathbf{\Lambda}^{(5)}\mathfrak{U})), \tag{22}$$

where the symbol $*$ represent element-wise multiplication of two vectors.

$$\begin{aligned}
\mathfrak{U} &= [U_1, U_2, U_3, \ldots, U_N]^T, \\
\mathbf{\Lambda}_{N\times N}^{(1)} &= [m_{pk}] = [\boldsymbol{\lambda}_k^{(1)}], k = p_1, p_2, \ldots, p_{n_p}, p = 2,3,\ldots,N-1, \\
\mathbf{\Lambda}_{N\times N}^{(2)} &= [m_{pk}] = [\boldsymbol{\lambda}_k^{(2)}], k = p_1, p_2, \ldots, p_{n_p}, p = 2,3,\ldots,N-1. \\
\mathbf{\Lambda}_{N\times N}^{(3)} &= [m_{pk}] = [\boldsymbol{\lambda}_k^{(3)}], k = p_1, p_2, \ldots, p_{n_p}, p = 2,3,\ldots,N-1. \\
\mathbf{\Lambda}_{N\times N}^{(5)} &= [m_{pk}] = [\boldsymbol{\lambda}_k^{(5)}], k = p_1, p_2, \ldots, p_{n_p}, p = 2,3,\ldots,N-1.
\end{aligned} \tag{23}$$

The corresponding initial condition is given as

$$\mathfrak{U}(t_0) = [U_0(x_1), U_0(x_2), \ldots, U_0(x_N)]^T. \tag{24}$$

## 4 Results and discussion

To check the accuracy and efficiency of the LMM various test problems in one and two dimensional cases are considered and the results are compared with the existence methods reported in literature. For spatial discretization three types of RBFs that is, MQ, IMQ and GA are used whereas for time integration have used explicit Euler method (EEM) and Runge-Kutta method of order 4 (RK4).

Accuracy of the LMM is measured though different error norms given as follows

$$\begin{aligned}
L_{abs} &= |U_{exact}(p) - U(p)|, \;\; p = 1,2,\ldots,N^n. \quad L_\infty = \max(L_{abs}), \\
L_2 &= \left[h\sum_{p=1}^{N} {L_{abs}}^2\right]^{\frac{1}{2}}, \quad L_{rms} = \left[\frac{1}{N}\sum_{p=1}^{N} {L_{abs}}^2\right]^{\frac{1}{2}},
\end{aligned} \tag{25}$$

where exact and numerical solution are represented by $U_{exact}$ and $U$ respectively.

Summary of numerical results is given as: Results of 1D fifth order KdV equation are shown in Table 1 and compared with the method in [8] whereas numerical results of seventh order KdV equation are presented in Table 2. Similarly the numerical results of generalized Burgers' Huxley equation are presented in Tables 3-4 and the results are compared with the methods given in [4, 11, 24, 29] while the numerical results of Huxley equation are shown in Tables 5-6 and compared with the methods in [5, 24, 29]. Numerical results of generalized Burgers' Fisher equation are shown in Table 7 and compared with the methods in [24, 29]. Numerical results of

Preprints (www.preprints.org) | NOT PEER-REVIEWED | Posted: 31 January 2019 doi:10.20944/preprints201901.0330.v1

Peer-reviewed version available at Mathematics 2019, 7, 216; doi:10.3390/math7030216

Table 1: **Numerical results the LMM for Test Problem 1.**

| $t$ | EEM | [8] | EEM | [8] | EEM | [8] | EEM | [8] |
|---|---|---|---|---|---|---|---|---|
| | x=0.2 | | x=0.6 | | x=1 | | x=5 | |
| 2 | 5.2899e-15 | 5.7619e-14 | 1.5870e-14 | 1.7278e-13 | 2.6450e-14 | 2.8786e-13 | 1.2669e-13 | 1.4210e-12 |
| 4 | 1.0580e-14 | 1.1528e-13 | 3.1740e-14 | 3.4561e-13 | 5.2900e-14 | 5.7577e-13 | 2.5337e-13 | 2.8421e-12 |
| 6 | 1.5869e-14 | 1.7298e-13 | 4.7610e-14 | 5.1848e-13 | 7.9350e-14 | 8.6372e-13 | 3.8006e-13 | 4.2632e-12 |
| 8 | 2.1159e-14 | 2.3073e-13 | 6.3479e-14 | 6.9140e-13 | 1.0580e-13 | 1.1517e-12 | 5.0676e-13 | 5.6844e-12 |
| 10 | 2.6448e-14 | 2.8851e-13 | 7.9349e-14 | 8.6435e-13 | 1.3225e-13 | 1.4397e-12 | 6.3345e-13 | 7.1056e-12 |

Table 2: **Numerical results in form of $L_\infty$ error norm using the EEM for Test Problem 2.**

| t | k=0.1 | k=0.01 | k=0.001 | CPU time (seconds) |
|---|---|---|---|---|
| 1 | 5.8157e-10 | 1.2395e-15 | 3.3881e-19 | 0.03 |
| 10 | 5.8205e-09 | 1.2395e-14 | 3.3881e-18 | 0.21 |
| 20 | 1.1652e-08 | 2.4790e-14 | 6.7763e-18 | 0.46 |
| 30 | 1.7494e-08 | 3.7185e-14 | 1.0164e-17 | 0.71 |
| 50 | 2.9211e-08 | 6.1975e-14 | 1.6941e-17 | 1.07 |

Fitzhugh-Nagumo equation are given in Table 8, Figs. 1-2 and the results are compared with the method reported in [26]. Numerical results of coupled KdV equations are presented in Tables 9 and the results are compared with the method given in [39] while numerical results of Hirota-Satsuma coupled KdV equation are shown in Table 10. Numerical simulation of reaction-diffusion Brusselator system are shown in Table 11 and comparison is made with the methods in [38, 46].

**Test Problem 1.** The exact solution [8] of the 1D Lax's fifth order KdV equation (1) is

$$U(x,t) = 2k^2\left(2 - 3\tanh^2\left(k(x - 56k^4t - x_0)\right)\right), \quad x \in [-10, 10], \quad t \geq 0 \tag{26}$$

where the initial and boundary conditions are extracted from the exact solution (26).
Numerical results for Test Problem 1 are given in Table 1 using $k = 0.01$, $x_0 = 0$, $dt = 0.01$, $N = 11$ and shape parameter $c = 100$. Table 1 indicated that the results produced by the LMM using EEM are more better than the method in [8].

**Test Problem 2.** The 1D Lax's seventh order KdV equation (2) having exact solution [12]

$$U(x,t) = 2k^2 sech^2\left(k(x - 64k^6t)\right), \quad x \in [-100, 100], \quad t \geq 0 \tag{27}$$

where the initial and boundary equations are extracted from the exact solution (27).
To demonstrate the accuracy and efficiency of the proposed LMM, we reported numerical results in Table 2 for Test Problem 2, in form of $L_\infty$ error norm using different values of $k$ and $t$. We have used EEM with $dt = 0.01$, $N = 11$ using MQ RBF ($c = 100$). From Table 2, one can observe that the LMM is accurate and efficient.

**Test Problem 3.** The 1D generalized Burgers' Huxley equation (3) having exact solution taken from [44] is given by

$$U(x,t) = \left(\frac{\gamma}{2} + \frac{\gamma}{2}\tanh\left(\omega_1(x - \omega_2 t)\right)\right)^{\frac{1}{\delta}}, \quad a \leq x \leq b, \quad t \geq 0, \tag{28}$$

Preprints (www.preprints.org) | NOT PEER-REVIEWED | Posted: 31 January 2019 doi:10.20944/preprints201901.0330.v1

Peer-reviewed version available at Mathematics 2019, 7, 216; doi:10.3390/math7030216

Table 3: **Numerical results of generalized Burgers' Huxley equation in term of $L_{abs}$ error norm using the RK4 for Test Problem 3.**

| $t$ | $x$ | RK4 | [29] | [24] | [4] |
|---|---|---|---|---|---|
| 0.05 | 0.1 | 6.30e-12 | 1.0e-09 | 1.93e-07 | 1.87e-08 |
| | 0.5 | 4.42e-12 | 1.0e-09 | 1.93e-07 | 1.87e-08 |
| | 0.9 | 2.55e-12 | 1.0e-09 | 1.93e-07 | 1.87e-08 |
| 0.1 | 0.1 | 1.23e-11 | 1.0e-09 | 3.87e-07 | 3.75e-08 |
| | 0.5 | 8.62e-12 | 1.0e-09 | 3.87e-07 | 3.75e-08 |
| | 0.9 | 4.87e-12 | 1.0e-09 | 3.87e-07 | 3.75e-08 |
| 1.0 | 0.1 | 8.16e-11 | 0.0e-09 | 3.88e-06 | 3.75e-07 |
| | 0.5 | 4.41e-11 | 0.0e-09 | 3.88e-06 | 3.75e-07 |
| | 0.9 | 6.61e-12 | 0.0e-09 | 3.88e-06 | 3.75e-07 |

where

$$\omega_1 = \frac{-\alpha\delta + \delta\sqrt{\alpha^2 + 4\beta(1+\delta)}}{4(1+\delta)}\gamma, \quad \omega_2 = \frac{\alpha\gamma}{1+\delta} - \frac{(1+\delta-\gamma)(-\alpha + \sqrt{\alpha^2 + 4\beta(1+\delta)})}{2(1+\delta)},$$

where $\alpha$, $\beta$, $\delta$ and $\gamma$ are constants such that $\beta \geq 0$, $\delta > 0$, $\gamma \in (0, 1)$.
In Table 3, we have compared the results obtained by the LMM for generalized Burgers' Huxley equation for Test Problem 3 with the methods given in [4, 24, 29]. We have used the parameters values $\alpha = \beta = \delta = 1$ and $\gamma = 0.001$ and time step length $dt = 0.0001$, spatial domain $[-10, 20]$, $N = 61$ using IMQ RBF. From Table 3, we have noted that the RK4 produced more accurate results than the results reported in [4, 24, 29]. Table 4 also shows the comparison of numerical results produced by the LMM with the results of Haar wavelet method given in [11]. In the table we have calculated the absolute errors for different values of $x$ and $\delta$ with $\alpha = \beta = 1$, $\gamma = 0.001$, and $t = 0.8$ using IMQ RBF. It can be observed from the table that the LMM is more accurate than the method reported in [11]. The numerical results of Huxley equation for Test Problem 3 with spatial domain $[-10, 20]$, $N = 61$, $dt = 0.01$ and different values of $x$ and $t$ are shown in Table 5. We have used IMQ radial basis function and $\beta = \delta = 1$, $\gamma = 0.001$. The numerical simulations have carried out by using the RK4 and comparison is done with [24, 29] in Table 5. From the table, we have noticed that the results produced by the LMM are better than the methods reported in [24, 29].

**Test Problem 4.** The exact solution [7] of the 1D Huxley equation (4) with $\alpha = \gamma = 1$ is given below as

$$U(x,t) = \frac{1}{2} + \frac{1}{2}\tanh\left(\frac{1}{2\sqrt{2}}(x - \frac{t}{\sqrt{2}})\right), \quad a \leq x \leq b, \quad t \geq 0, \tag{29}$$

The numerical simulations have carried out for Test Problem 4 in Table 6 for different values of $t$, $x$, $a$, $b$ and for $N = 10$, $dt = 0.0001$ using MQ RBF with $c = 5$. The results are obtained by the EEM and compared with the results obtained by Chebyshev spectral collocation method in [5] and found that the results of the LMM are superior.

Preprints (www.preprints.org) | NOT PEER-REVIEWED | Posted: 31 January 2019 doi:10.20944/preprints201901.0330.v1

Peer-reviewed version available at Mathematics 2019, 7, 216; doi:10.3390/math7030216

Table 4: **Numerical results in form of $L_{abs}$ error norm using the RK4 for Test Problem 3.**

| $x$ | RK4 $\delta = 1$ | [11] $\delta = 1$ | RK4 $\delta = 2$ | [11] $\delta = 2$ |
|---|---|---|---|---|
| 0.03125 | 7.7951e-11 | 5.595048500e-09 | 5.9126e-07 | 2.60170e-07 |
| 0.09375 | 7.3263e-11 | 1.585754820e-08 | 5.9089e-07 | 7.37310e-07 |
| 0.15625 | 6.8575e-11 | 2.464804780e-08 | 5.9052e-07 | 1.14654e-06 |
| 0.21875 | 6.3887e-11 | 3.197174720e-08 | 5.9015e-07 | 1.48748e-06 |
| 0.28125 | 5.9200e-11 | 3.783204670e-08 | 5.8977e-07 | 1.76007e-06 |
| 0.34375 | 5.4512e-11 | 4.222624610e-08 | 5.8940e-07 | 1.96449e-06 |
| 0.40625 | 4.9824e-11 | 4.515634540e-08 | 5.8903e-07 | 2.10047e-06 |
| 0.46875 | 4.5137e-11 | 4.662174470e-08 | 5.8866e-07 | 2.17497e-06 |
| 0.53125 | 4.0448e-11 | 4.662274380e-08 | 5.8828e-07 | 2.17497e-06 |
| 0.59375 | 3.5759e-11 | 4.515724300e-08 | 5.8791e-07 | 2.10054e-06 |
| 0.65625 | 3.1070e-11 | 4.222824200e-08 | 5.8754e-07 | 1.96433e-06 |
| 0.71875 | 2.6382e-11 | 3.783454090e-08 | 5.8717e-07 | 1.76033e-06 |
| 0.78125 | 2.1693e-11 | 3.197443970e-08 | 5.8680e-07 | 1.48745e-06 |
| 0.84375 | 1.7004e-11 | 2.465083840e-08 | 5.8642e-07 | 1.14629e-06 |
| 0.90625 | 1.2315e-11 | 1.586053710e-08 | 5.8605e-07 | 7.37610e-07 |
| 0.96875 | 7.6260e-12 | 5.596235600e-09 | 5.8568e-07 | 2.60370e-07 |

Table 5: **Comparison of Huxley equation in term of $L_{abs}$ error norm using the RK4 for Test Problem 3.**

| $t$ | $x$ | RK4 | [29] | [24] |
|---|---|---|---|---|
| 0.05 | 0.1 | 2.18e-11 | 0.0e-09 | 1.88e-07 |
| | 0.5 | 1.83e-11 | 1.0e-09 | 1.87e-07 |
| | 0.9 | 1.47e-11 | 1.0e-09 | 1.87e-07 |
| 0.1 | 0.1 | 4.29e-11 | 1.0e-09 | 3.75e-07 |
| | 0.5 | 3.59e-11 | 0.0e-09 | 3.75e-07 |
| | 0.9 | 2.88e-11 | 0.0e-09 | 3.75e-07 |
| 1.0 | 0.1 | 3.18e-10 | 1.0e-09 | 3.75e-06 |
| | 0.5 | 2.47e-10 | 0.0e-09 | 3.75e-06 |
| | 0.9 | 1.76e-10 | 1.0e-09 | 3.75e-06 |

Table 6: **Comparison of Huxley equation in term of $L_{abs}$ error norm using the EEM for Test Problem 4.**

| $a$ | $b$ | $t$ | $x$ | $L_{abs}$ | $L_{abs}$ [5] |
|---|---|---|---|---|---|
| -2 | 2 | 0.002 | 0.050 | 1.9974e-07 | 2.22e-03 |
| -2 | 2 | 0.100 | 0.700 | 3.0067e-06 | 1.78e-03 |
| -5 | 5 | 0.001 | 0.500 | 2.5260e-07 | 1.69e-02 |
| -5 | 5 | 0.001 | 2.500 | 1.7843e-06 | 9.90e-03 |
| -10 | 10 | 0.002 | 0.010 | 3.6673e-06 | 4.05e-04 |
| -10 | 10 | 0.100 | 1.000 | 2.7722e-04 | 3.17e-03 |

Preprints (www.preprints.org) | NOT PEER-REVIEWED | Posted: 31 January 2019 doi:10.20944/preprints201901.0330.v1

Peer-reviewed version available at Mathematics 2019, 7, 216; doi:10.3390/math7030216

Table 7: **Numerical results of generalized Burgers' Fisher equation in term of $L_{abs}$ error norm using the RK4 for Test Problem 5.**

| $t$ | $x$ | RK4 | $L_{abs}$ [29] | $L_{abs}$ [24] |
|---|---|---|---|---|
| 0.005 | 0.1 | 3.2492e-08 | 2.7e-07 | 9.75e-06 |
| | 0.5 | 3.2495e-08 | 1.4e-07 | 5.96e-05 |
| | 0.9 | 3.2498e-08 | 2.7e-07 | 9.75e-06 |
| 0.01 | 0.1 | 2.4835e-09 | 2.7e-07 | 1.90e-05 |
| | 0.5 | 2.4895e-09 | 1.3e-07 | 1.90e-05 |
| | 0.9 | 2.4955e-09 | 2.7e-07 | 1.90e-05 |

**Test Problem 5.** The exact solution of the 1D generalized Burgers' Fisher equation (5) is given below as

$$U(x,t) = \left(\frac{1}{2} + \frac{1}{2}\tanh(a_1(x - a_2 t))\right)^{\frac{1}{\delta}}, \quad a \le x \le b, \quad t \ge 0, \tag{30}$$

where

$$a_1 = \frac{-\alpha\delta}{2(1+\delta)}, \quad a_2 = \frac{\alpha}{1+\delta} + \frac{\beta(1+\delta)}{\alpha}. \tag{31}$$

Numerical results of the LMM using the RK4 for Test Problem 5 is reported in Table 7. To verify the accuracy of the LMM, we have compared the results with the global meshless collocation method based on RBFs [29] and Adomian decomposition method [24]. The absolute errors for different $t$, $x$ and $N = 41$, $dt = 0.001$, $\alpha = \beta = 0.001$, $\delta = 1$, spatial domain $[-20, 20]$ using IMQ RBF are given in Table 7. From the table, one can ensure that the results of the LMM are more accurate than the methods given in [24, 29].

**Test Problem 6.** The exact solution [26] of the 1D nonlinear standard Fitzhugh-Nagumo equation (6) is

$$U(x,t) = \frac{1}{2} + \frac{1}{2}\tanh\left(\frac{1}{2\sqrt{2}}(x - \frac{2\rho - 1}{\sqrt{2}}t)\right), \quad x \in [-10, 10] \quad t \ge 0. \tag{32}$$

In Table 8 we have calculated numerical results for Test Problem 6 with $N = 101$, $dt = 0.0001$ using MQ RBF. Table 8 shows $L_{rms}$ and $L_\infty$ error norms of the EEM for $q = 0.75$. From the table it can be seen that the obtained results are quite agreed with the results given in [26]. Fig. 1 shows the comparison of numerical and analytical solutions for $t = 0.2, 0.4, 0.6, 0.8, 1$, $q = 4$ and $N = 41$ for Test Problem 6 while Fig. 2 shows the numerical simulations of the EEM for $q = 0.75$ and $q = 4$.

**Test Problem 7.** The exact solution [39] of 1D coupled KdV equation (7) with $\gamma = 3$ and $\alpha = \beta$ is

$$U(x,t) = \frac{\lambda}{\alpha} sech^2\left(\frac{1}{2}\sqrt{\frac{\lambda}{\alpha}}(x - \lambda t)\right), \quad V(x,t) = \frac{\sqrt{\frac{1}{\alpha}}\lambda sech^2\left(\frac{1}{2}\sqrt{\frac{\lambda}{\alpha}}(x - \lambda t)\right)}{\sqrt{2}}. \tag{33}$$

Preprints (www.preprints.org) | NOT PEER-REVIEWED | Posted: 31 January 2019 doi:10.20944/preprints201901.0330.v1

Peer-reviewed version available at Mathematics 2019, 7, 216; doi:10.3390/math7030216

Table 8: **Comparison of FN equation using the EEM for Test Problem 6.**

| $t$ | $L_\infty$ | $L_{rms}$ | $L_\infty$ [26] | $L_{rms}$ [26] |
|---|---|---|---|---|
| 0.2 | 1.8896e-05 | 2.1960e-07 | 4.7416e-05 | 1.5880e-05 |
| 0.5 | 4.1554e-05 | 1.5696e-06 | 1.2312e-04 | 3.8433e-05 |
| 1.0 | 6.9891e-05 | 7.1449e-06 | 2.6261e-04 | 8.1870e-05 |
| 1.5 | 9.1687e-05 | 1.7262e-05 | 4.2096e-04 | 1.3387e-04 |
| 2.0 | 1.0969e-04 | 3.1857e-05 | 5.9999e-04 | 1.9433e-04 |
| 3.0 | 1.3942e-04 | 7.2878e-05 | 1.0324e-03 | 3.4320e-04 |
| 5.0 | 1.8964e-04 | 1.8803e-04 | 2.3050e-03 | 7.8638e-04 |

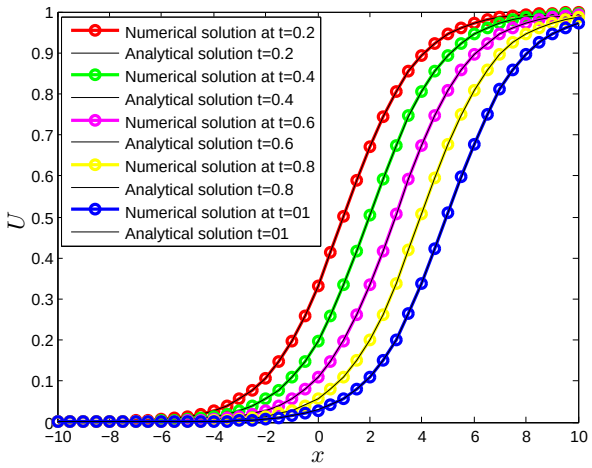


Figure 1: Comparing the curves of the numerical and analytical solutions for $N = 41$, $q = 4$ for Test Problem 6.

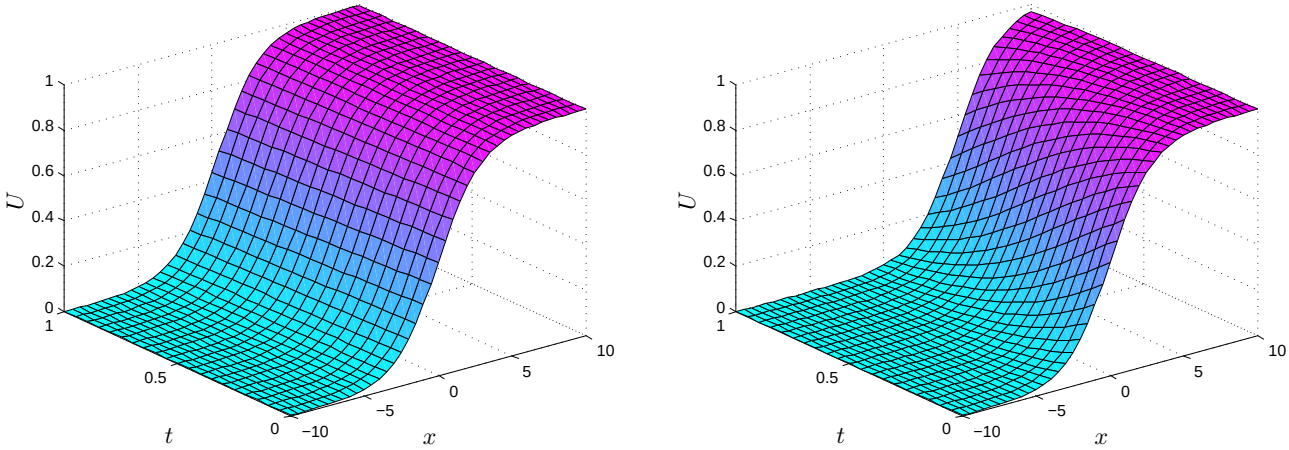


Figure 2: (Left) Numerical solutions for $q = 0.75$, (Right) Numerical solutions for $q = 4$ using the EEM for $N = 41$, $t = 1$ for Test Problem 6.

In Table 9, we have listed numerical simulations of the EEM versus results obtained from RBFs based collocation method [39] for Test Problem 7. The value of the parameters are $\alpha = \beta = \lambda = 0.01$ with the spatial domain $[-5, 5]$, $N = 101$, $dt = 0.001$ and for various time $t$, using MQ radial

Preprints (www.preprints.org) | NOT PEER-REVIEWED | Posted: 31 January 2019 doi:10.20944/preprints201901.0330.v1

Peer-reviewed version available at Mathematics 2019, 7, 216; doi:10.3390/math7030216

Table 9: **Numerical results of coupled KdV system in form of $L_2$ error norm using the EEM for Test Problem 7.**

| t | 0.1 | 0.2 | 0.3 | 0.4 | 0.5 | 1 | 2 |
|---|---|---|---|---|---|---|---|
| [39] | | | | | | | |
| U | 3.662e-05 | 5.177e-05 | 4.065e-05 | 3.951e-05 | 3.964e-05 | 3.975e-05 | 4.461e-05 |
| V | 2.584e-06 | 3.648e-06 | 2.855e-06 | 2.769e-06 | 2.772e-06 | 2.749e-06 | 3.033e-06 |
| EEM | | | | | | | |
| U | 8.3147e-08 | 3.3251e-07 | 7.4809e-07 | 1.3299e-06 | 2.0779e-06 | 8.3112e-06 | 3.3245e-05 |
| V | 5.8794e-09 | 2.3512e-08 | 5.2898e-08 | 9.4037e-08 | 1.4693e-07 | 5.8769e-07 | 2.3508e-06 |

Table 10: **Numerical results of the EEM for Test Problem 8.**

| | EEM | | | |
|---|---|---|---|---|
| | $L_\infty$ | | | |
| $k$ | $t$ | U | V | W |
| 0.1 | 0.25 | 4.9097e-05 | 1.7702e-08 | 1.7702e-08 |
| | 0.5 | 9.8195e-05 | 3.6410e-08 | 3.6410e-08 |
| | 0.75 | 1.4729e-04 | 5.6117e-08 | 5.6117e-08 |
| | 1.0 | 1.9639e-04 | 7.6814e-08 | 7.6814e-08 |
| | 5.0 | 9.8258e-04 | 6.0675e-07 | 6.0675e-07 |
| 0.05 | 0.25 | 5.2245e-06 | 2.2740e-09 | 2.2740e-09 |
| | 0.5 | 1.0464e-05 | 4.5679e-09 | 4.5679e-09 |
| | 0.75 | 1.5720e-05 | 6.8820e-09 | 6.8820e-09 |
| | 1.0 | 2.0991e-05 | 9.2162e-09 | 9.2162e-09 |
| | 5.0 | 1.0741e-04 | 4.9335e-08 | 4.9335e-08 |

basis function with $c = 100$. From the listed results given in Table 9, we have observed that the results obtained by the EEM are better than the results given in [39].

**Test Problem 8.** The 1D Hirota-Satsuma coupled KdV system (8) with exact solution [28] given below

$$\begin{aligned} U(x,t) &= 4k^2q_2\tanh^2(\xi) - \frac{8k^2q_2}{3} - \frac{C}{3}, \\ V(x,t) &= 2k^2q_2\tanh^2(\xi) - \frac{2k^2q_2}{3} - \frac{4}{3} - c_0, \\ W(x,t) &= 2k^2q_2\tanh^2(\xi) - 2k^2q_2 + c_0. \end{aligned} \tag{34}$$

where $\xi = \sqrt{q_2}k(x - Ct)$ and $a \le x \le b$. In Table 10 the numerical simulations of Hirota-Satsuma coupled KdV system (8) are carried out for Test problem 8 on the interval $[-30, 30]$ and different values of $k$ and $t$, with $N = 13$, $dt = 0.05$, using MQ RBF with $c = 2$. The value of parameters $C = c_0 = q_2 = 0.1$. A full agreement between numeric and exact solution have been observed.

**Test Problem 9.** The analytic solution of the 2D reaction-diffusion Brusselator system (9) for

Preprints (www.preprints.org) | NOT PEER-REVIEWED | Posted: 31 January 2019 doi:10.20944/preprints201901.0330.v1

Peer-reviewed version available at Mathematics 2019, 7, 216; doi:10.3390/math7030216

Table 11: **Comparison of numerical results of the EEM using GA RBF at point** $(0.40, 0.60)$ **for Test Problem 9.**

| | | $U$ | | | | $V$ | | | |
|---|---|---|---|---|---|---|---|---|---|
| t | CPU time | EEM | [38] | [46] | Exact | EEM | [38] | [46] | Exact |
| 0.30 | 0.17 | 0.3167 | 0.3168 | 0.3166 | 0.3166 | 3.1584 | 3.158 | 3.157 | 3.158 |
| 0.60 | 0.19 | 0.2726 | 0.2724 | 0.2725 | 0.2725 | 3.6696 | 3.669 | 3.667 | 3.669 |
| 0.90 | 0.23 | 0.2346 | 0.2347 | 0.2345 | 0.2346 | 4.2635 | 4.263 | 4.260 | 4.263 |
| 1.20 | 0.26 | 0.2019 | 0.2020 | 0.2018 | 0.2019 | 4.9534 | 4.953 | 4.950 | 4.953 |
| 1.50 | 0.30 | 0.1738 | 0.1739 | 0.1737 | 0.1738 | 5.7551 | 5.755 | 5.751 | 5.755 |
| 1.80 | 0.34 | 0.1496 | 0.1496 | 0.1495 | 0.1496 | 6.6864 | 6.686 | 6.681 | 6.686 |

a particular case in the region $(x, y) \in [0, 1]^2$, $t \geq 0$ with $\alpha = 1$, $\beta = 0$, $\gamma = 0.25$ is given in [46]

$$U(x, y, t) = \exp\left(-x - y - \frac{t}{2}\right), \quad V(x, y, t) = \exp\left(x + y + \frac{t}{2}\right). \tag{35}$$

The LMM is employed for the numerical solution of Test Problem 9 by letting time step length $dt = 0.001$, the shape parameter value $c = 1$, $N = 20 \times 20$, at various times up to $t = 1.8$. In Table 11 we have compared the results obtained by the EEM with the exact solution as well as with [38, 46]. Reasonably good accuracy has been obtained in this case as well also CPU time in seconds are reported in the same table. The numerical results on irregular domains are shown in Figs. 3-6 for Test Problem 9 using MQ RBF with shape parameter $c = 1$. The numerical solutions shown in Figs. 3-6 are performed with $dt = 0.001$, $t = 1$ $\alpha = 1$, $\beta = 0$ and $\mu = 0.25$. These figures show the efficiency of the suggested method in irregular geometry in term of absolute error $L_{abs}$ by using the EEM for Test Problem 9.

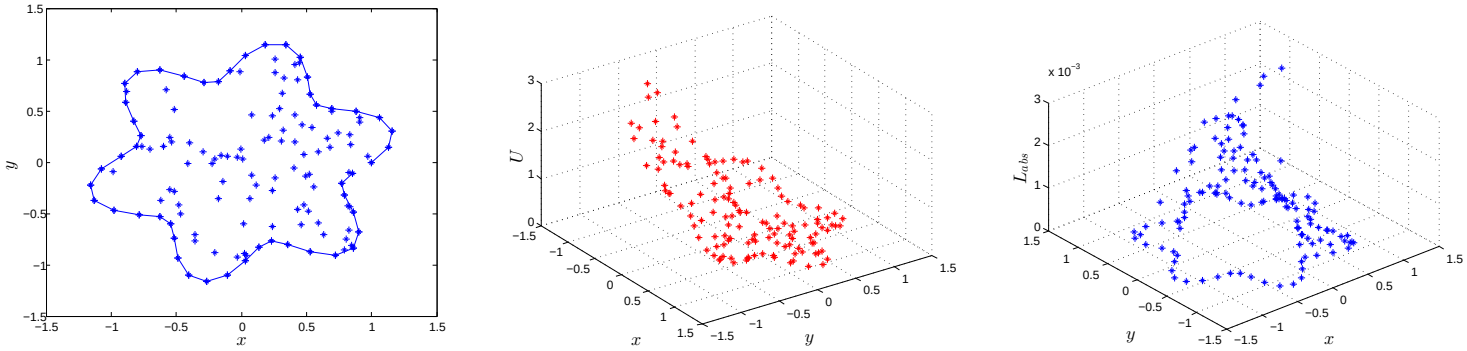


Figure 3: Computational domain, numerical solution and absolute error by using the EEM for Test Problem 9.

Preprints (www.preprints.org) | NOT PEER-REVIEWED | Posted: 31 January 2019 doi:10.20944/preprints201901.0330.v1

Peer-reviewed version available at Mathematics 2019, 7, 216; doi:10.3390/math7030216

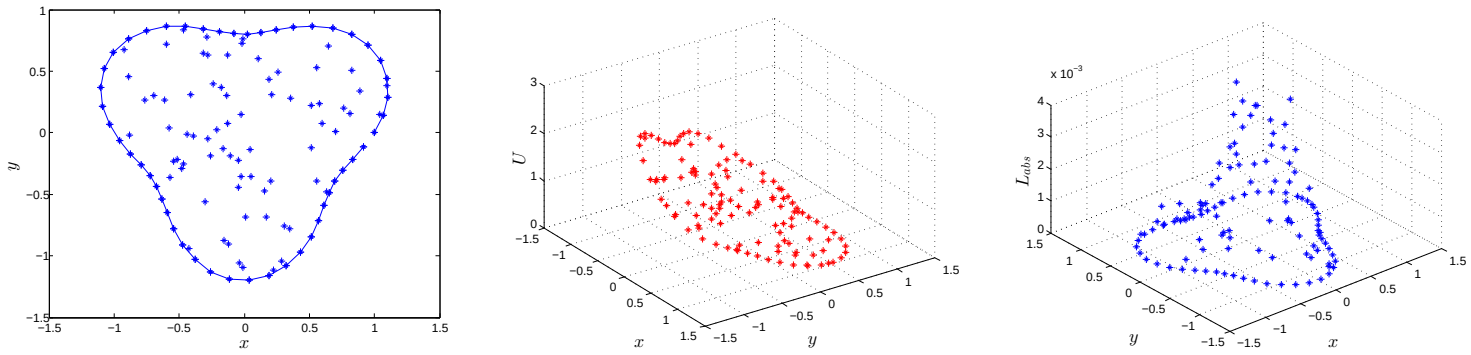


Figure 4: Computational domain, numerical solution and absolute error by using the EEM for Test Problem 9.

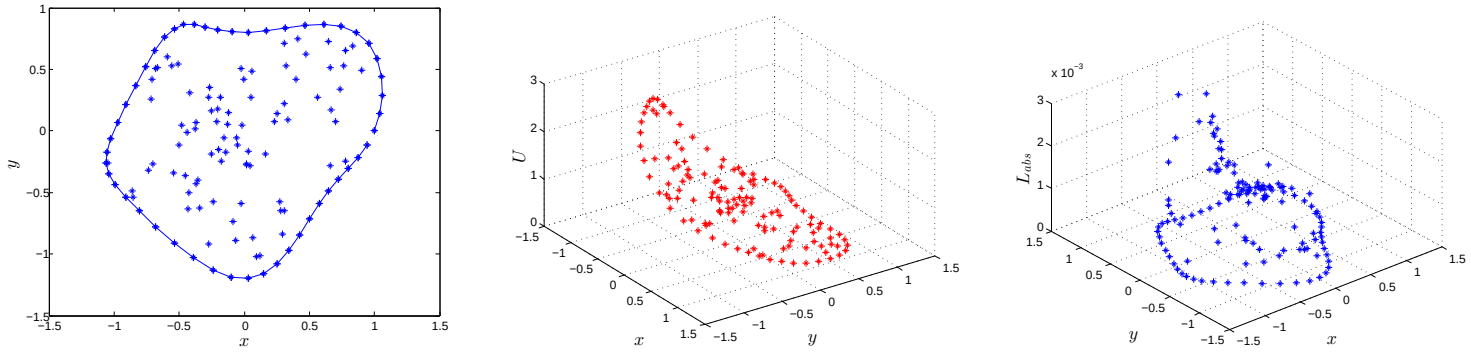


Figure 5: Computational domain, numerical solution and absolute error by using the EEM for Test Problem 9.

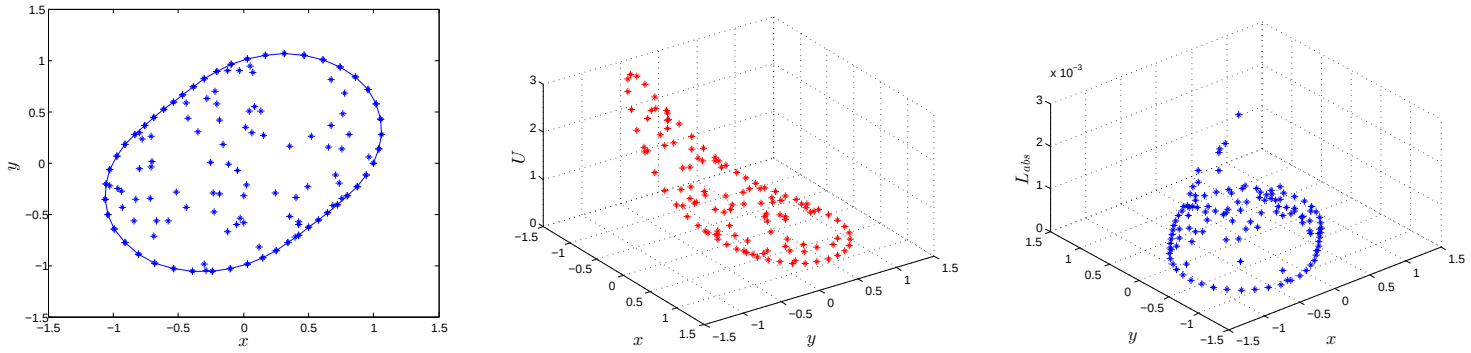


Figure 6: Computational domain, numerical solution and absolute error by using the EEM for Test Problem 9.

## 5 Conclusion

In this work, a local meshless differential quadrature collocation method is proposed for numerical solution of different mathematical models arising in science and engineering. These models have been solved in the literature by using various numerical methods. To check the accuracy and efficacy of the proposed scheme on both regular and irregular domains different test problems have been considered. Results of the local meshless method are compared with exact/approximate

solutions available in the existence literature. On the basis of these results/ comparison we can conclude that the local meshless method is accurate, efficient and its implementation is very simple, straightforward, irrespective of the dimension and geometry of the problem.

## Acknowledgements

This project was supported by the Theoretical and Computational Science (TaCS) Center under Computational and Applied Science for Smart Innovation Cluster (CLASSIC), Faculty of Science, KMUTT.

## References

[1] S. Abbasbandy. Soliton solutions for the Fitzhugh-Nagumo equation with the homotopy analysis method. *Applied Mathematical Modelling*, 32:2706–2714, 2008.

[2] G. Adomian. The diffusion Brusselator equation. *Computers and Mathematics with Applications*, 29:1–3, 1995.

[3] Imtiaz Ahmad, Siraj-ul-Islam, and Abdul Q. M. Khaliq. Local RBF method for multi-dimensional partial differential equations. *Computers and Mathematics with Applications*, 74:292–324, 2017.

[4] A. M. Al-Rozbayani and M. O. Al-Amr. Discrete adomian decomposition method for solving Burgers'-Huxley equation. *International Journal of Contemporary Mathematical Sciences*, 8:623–631, 2013.

[5] S. Ashrafi, M. Alineia, H. Kheiri, and G. Hojjati. Spectral collocation method for the numerical solution of the Gardner and Huxley equations. *International Journal of Nonlinear Science*, 18:71–77, 2014.

[6] L. M. B. Assas. Variational iteration method for solving coupled-KdV equations. *Chaos, Solitons and Fractals*, 38:1225–1228, 2008.

[7] E. Babolian and J. Saeidian. Analytic approximate solutions to Burgers', Fisher, Huxley equations and two combined forms of these equations. *Communications in Nonlinear Science and Numerical Simulation*, 14:1984–1992, 2009.

[8] H. O. Bakodah. Modified Adomain Decomposition Method for the generalized fifth order KdV equations. *American Journal of Computational Mathematics*, 3:53–58, 2013.

[9] A. H. Bhrawy. A Jacobi-Gauss-Lobatto collocation method for solving generalized Fitzhugh-Nagumo equation with time-dependent coefficients. *Applied Mathematics and Computation*, 222:255–264, 2013.

[10] M. Bukhari, M. Arshad, S. Batool, and S. M. Saqlain. Numerical solution of generalized Burger's-Huxley equation using local radial basis functions. *International Journal of Advanced and Applied Sciences*, 4(5):1–11, 2017.

[11] I. Celik. Haar wavelet method for solving generalized Burgers'-Huxley equation. *Arab Journal of Mathematical Sciences*, 18:25–37, 2012.

[12] M. T. Darvishia, S. Kheybari, and F. Khani. A numerical solution of the Lax's 7th-order KdV equation by Pseudospectral method and Darvishi's preconditioning. *International Journal of Contemporary Mathematical Sciences*, 2:1097–1106, 2007.

[13] K. Djidjeli, W. G. Price, E. H. Twizell, and Y. Wang. Numerical methods for the soltution of the third and fifth-order disprsive Korteweg-de Vries equations. *Journal of Computation-aland Applied Mathematics*, 58:307–336, 1995.

[14] S. M. El-Sayed and D. Kaya. An application of the ADM to seven-order Sawada-Kotara equations. *Applied Mathematics and Computation*, 157:93–104, 2004.

[15] R. A. Fisher. The Wave of Advance of Advantageous Genes. *Annals of Eugenics*, 7:355–369, 1937.

[16] R. FitzHugh. Impulses and physiological states in theoretical models of nerve membrane. *Biophysical journal*, 1:445–466, 1961.

[17] D. D. Ganji, M. Nourollahi, and M. Rostamian. A comparison of Variational Iteration Method with Adomian's Decomposition Method in some highly nonlinear equations. *International Journal of Science and Technology*, 2:179–188, 2007.

[18] A. Goswami, J. Singh, and D. Kumar. Numerical simulation of fifth order KdV equations occurring in magneto-acoustic waves. *Ain Shams Engineering Journal*, 2017.

[19] Sirajul Haq, A. Hussain, and M. Uddin. RBFs meshless method of lines for the numerical solution of time-dependent nonlinear coupled partial differential equations. *Applied Mathematics*, 2:414–423, 2011.

[20] G. Hariharan and K. Kannan. Haar wavelet method for solving Fitzhugh-Nagumo equation. *World Academy of Science*, 43:560–564, 2010.

[21] M. A. Helal and M. S. Mehanna. A comparative study between two different methods for solving the general Korteweg-de Vries equation (GKDV). *Chaos, Solitons and Fractals*, 33:725–739, 2007.

[22] R. Hirota and J. Satsuma. Soliton solutions of a coupled Kortewege-de Vries equation. *Physics Letters A*, 85:407–418, 1981.

[23] A. L. Hodgkin and A. F. Huxley. A quantitative description of Ion currents and its applications to conduction and excitation in nerve membranes. *Journal of Physiology*, 117:500–544, 1952.

[24] H. N. A. Ismail, K. R. Raslan, and A. A. A. Rabboh. Adomian decomposition method for Burgers'-Huxley and Burgers'-Fisher equations. *Applied Mathematics and Computation*, 159:291–301, 2004.

[25] M. Javidi. Modified pseudospectral method for generalized Burgers'-Fisher equation. *International Mathematical Forum*, 32:1555–1564, 2006.

[26] Ram Jiwari, R. K. Gupta, and Vikas Kumar. Polynomial differential quadrature method for numerical solutions of the generalized Fitzhugh-Nagumo equation with time-dependent coefficients. *Ain Shams Engineering Journal*, 5:1343–1350, 2014.

[27] D. Kaya. An explicit and numerical solutions of some fifth-order KdV equation by decomposition method. *Applied Mathematics and Computation*, 144:353–363, 2003.

[28] A. H. Khater, R. S. Temsah, and D. K. Callebaut. Numerical solutions for some coupled nonlinear evolution equations by using spectral collocation method. *Mathematical and Computer Modelling*, 48:1237–1253, 2008.

[29] A. J. Khattak. A computational meshless method for the generalized Burgers'-Huxley equation. *Applied Mathematical Modelling*, 33:3718–3729, 2009.

[30] R. Lefever and G. Nicolis. Chemical instabilities and sustained oscillations. *Journal of Theoretical Biology*, 30:267284, 1971.

[31] R. C. Mittal and A. Tripathi. Numerical solutions of generalized Burgers–Fisher and generalized Burgers–Huxley equations using collocation of cubic B-splines. *International Journal of Computer Mathematics*, 92(5):1053–1077, 2015.

[32] Mahdi Moghimia and Fatemeh S. A. Hejazi. Variational iteration method for solving generalized Burgers'-Fisher and Burgers' equations. *Chaos, Solitons and Fractals*, 33:1756–1761, 2007.

[33] J. S. Nagumo, S. Arimoto, and S. Yoshizawa. An active pulse transmission line simulating nerve axon. *Proceedings of the IRE*, 50:2061–2070, 1962.

[34] Y. Pomeau, A. Ramani, and B. Grammaticos. Structural stability of the Korteweg-de Vries solitons under a singular perturbation. *Physica D*, 31:127–134, 1988.

[35] J. Satsuma. Topics in soliton theory and exactly solvable nonlinear equations. *World Scientific, Singapore*, 1987.

[36] Siraj-ul-Islam and Imtiaz Ahmad. A comparative analysis of local meshless formulation for multi-asset option models. *Engineering Analysis with Boundary Elements*, 65:159–176, 2016.

[37] Siraj-ul-Islam and Imtiaz Ahmad. Local meshless method for PDEs arising from models of wound healing. *Applied Mathematical Modelling*, 48:688–710, 2017.

[38] Siraj-ul-Islam, A. Ali, and Sirajul Haq. A computational modeling of the behavior of the two-dimensional reaction-diffusion Brusselator system. *Applied Mathematical Modelling*, 34:3896–3909, 2010.

[39] Siraj-ul-Islam, Sirajul Haq, and Marjan Uddin. A meshfree interpolation method for the numerical solution of the coupled nonlinear partial differential equations. *Engineering Analysis with Boundary Elements*, 33:399–409, 2009.

[40] A. A. Soliman. A numerical simulation and explicit solutions of KdVBurgers' and lax's seventh-order KdV equations. *Chaos, Solitons and Fractals*, 29:294–302, 2006.

[41] P. Thounthong, M. N. Khan, I. Hussain, I. Ahmad, and P. Kumam. Symmetric radial basis function method for simulation of elliptic partial differential equations. *Mathematics*, 6(12):327, 2018.

[42] J. Tyson. Some further studies of nonlinear oscillations in chemical systems. *The Journal of Chemical Physics*, 58:3919, 1973.

[43] M. Uddin and Siraj ul Haq. Application of a numerical method using radial basis functions to nonlinear partial differential equations. *Selcuk Journal of Applied Mathematics*, 12:77–93, 2011.

[44] X. Y. Wang, Z. S. Zhu, and Y. K. Lu. Solitary wave solutions of the generalized Burgers'-Huxley equation. *Journal of Physics A: Mathematical and Theoretical*, 23:271–274, 1990.

[45] A. M. Wazwaz. The decomposition method applied to systems of partial differential equations and to the reaction-diffusion Brusselator model. *Applied Mathematics and Computation*, 110:251–264, 2000.

[46] Ang Whye-Teong. The two-dimensional reaction-diffusion Brusselator system: a dual-reciprocity boundary element solution. *Engineering Analysis with Boundary Elements*, 27:897–903, 2003.

[47] Y. T. Wu, X. G. Geng, X. B. Hu, and S. M. Zhu. Generalized Hirota-Satsuma coupled Korteweg-de Vries equation and Miura transformations. *Physics Letters A*, 64:255–259, 1999.

[48] Y. Yamaoto and E. Takizawa. On a solution on non-linear time-evolution equation of fifth-order. *Journal of the Physical Society of Japan*, 50, 1981.